Flexible Genetic Algorithm: A Simple and Generic Approach to Node Placement Problems ☆

Yu-Hui Zhang[a,b], Yue-Jiao Gong[b,*], Tian-Long Gu[c], Yun Li[d], Jun Zhang[b,*]

[a] *School of Data and Computer Science, Sun Yat-sen University, Guangzhou, China*
[b] *School of Computer Science and Engineering, South China University of Technology, Guangzhou, China*
[c] *Guilin University of Electronic Technology, Guilin, China*
[d] *School of Engineering, University of Glasgow, Glasgow, U.K.*

Abstract

Node placement problems, such as the deployment of radio-frequency identification systems or wireless sensor networks, are important problems encountered in various engineering fields. Although evolutionary algorithms have been successfully applied to node placement problems, their fixed-length encoding scheme limits the scope to adjust the number of deployed nodes optimally. To solve this problem, we develop a flexible genetic algorithm in this paper. With variable-length encoding, subarea-swap crossover, and Gaussian mutation, the flexible genetic algorithm is able to adjust the number of nodes and their corresponding properties automatically. Offspring (candidate layouts) are created legibly through a simple crossover that swaps selected subareas of parental layouts and through a simple mutation that tunes the properties of nodes. The flexible genetic algorithm is generic and suitable for various kinds of node placement problems. Two typical real-world node placement problems, i.e., the wind farm layout optimization and radio-frequency identification network planning problems, are used to investigate the performance of the proposed algorithm. Experimental results show that the flexible genetic algorithm offers higher performance than existing tools for solving node placement problems.

Keywords: genetic algorithm (GA), node placement problem (NPP), RFID network planning (RNP), variable-length encoding, wind farm layout optimization (WFLO)

☆This work was supported in part by the National Natural Science Foundation of China (NSFC) Key Project under Grant 61332002, in part by the NSFC Youth Project under Grant 61502542, and in part by the NSFC Joint Fund with Guangdong Key Projects under Grant U1201258.

*Corresponding author

Email addresses: gongyuejiao@gmail.com (Yue-Jiao Gong), junzhang@ieee.org (Jun Zhang)

1. Introduction

The node placement problem (NPP) is an important problem in many fields, such as radio frequency identification (RFID) [1], wireless sensor networks (WSNs) [2], wind farm design [3], and oil and gas industry [4]. The task of an NPP solver is to place a number of nodes optimally in a given area to meet certain predefined objectives. For this, there are mainly three issues to be addressed: 1) the number of nodes being deployed; 2) the positions of the nodes; 3) their property settings.

NPPs have been studied separately in the literature. They have different names in different contexts. For example, in the field of WSNs, an NPP is sometimes referred to as a 'relay node placement problem' [2, 5–8]. In other fields, specific terms such as RFID network planning (RNP) [1, 9–12], wind farm layout optimization (WFLO) [3, 13–16], and well placement optimization (WPO)[4, 17–19] problems are used. The definitions of the problems are different, but have something in common. Noticing that a solver to one of the problems may be applicable to the others with similar characteristics, this paper considers the problems in a generic prospective. To this end, we provide a general framework for NPPs and develop an approach capable of solving various NPP instances.

During the past decade, a substantial amount of research has been undertaken to address *ad hoc* NPPs. One sort of approach is to use deterministic algorithms such as integer linear programming [20, 21], mixed integer programming [22, 23], geometric programming [24], and some other approximation algorithms [6, 8, 25]. These algorithms are designed for particular problems with precise models. The defect is that the strong assumptions made by the models narrow the scope of application of the algorithms. On the other hand, an NPP is usually coupled with a series of constraints and has multiple objectives. These make the problem complex. As an example, the planning of RFID systems has been proven to be NP-Complete [26, 27].

Recently, the use of alternative methods such as heuristic [7], evolutionary algorithms (EAs) [28, 29] and swarm intelligence (SI) [30] has attracted an increasing attention. In the literature, both EAs such as genetic algorithms (GAs) [31–36] and SI techniques such as particle swarm optimization (PSO) [10, 11, 37] have been utilized to tackle *ad hoc* NPPs. However, since an EA uses a fixed-length encoding scheme to represent a candidate solution, it is hard to adjust the number of nodes.

To illustrate this, suppose a square area is given to place a number of nodes to meet predefined requirements. Fig. 1 shows the fixed-length encoding scheme used in [11, 31, 37–40], where n stands for the estimated number of nodes, and (x_i, y_i) and p_i represent the coordinates and property setting of the i-th node respectively. However, it is difficult to accurately estimate the number of nodes in need, which plays a vital role in the assessment of layouts. Hence, the deployment in [11, 31, 37–40] still has room to improve. An alternative is a grid-based binary encoding approach as used in [10, 13, 15, 32–36], which divides the target area into multiple grids and uses a binary variable to indicate

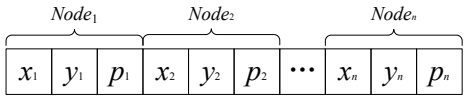

Figure 1: Fixed-length encoding scheme.

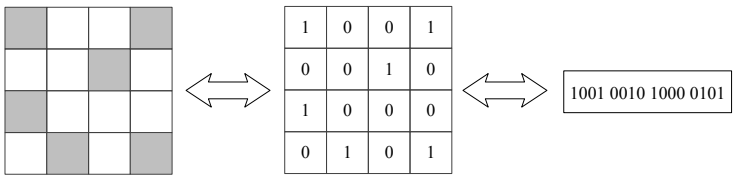

Figure 2: Grid-based method and its encoding scheme.

whether to place a node in the center of the corresponding grid, as shown in Fig. 2. In this way, a candidate solution (layout) can be represented by a binary string in a GA or PSO [41] to handle NPPs.

Although the grid-based approach is capable of pruning the number of nodes, there are two disadvantages. First, because the positions of the nodes are confined to the centers of the grids, the layout can only be optimized at a coarse-grained level. Second, it is inconvenient to incorporate additional properties of nodes (such as the transmitted power of RFID readers [12]) into the optimization process.

To optimize the number of nodes as well as the deployment, a variable length encoding scheme is required. In the literature, research efforts have been devoted to the design of variable length representations. One prominent research is the messy GA (mGA) proposed by Goldberg *et al.* [42]. Suppose the solution to a problem consists of n-bits. The algorithm allows the chromosome length to be larger or less than n. When evaluating the fitness of an individual, additional processing is used to interpret the chromosome if its length is not exactly n. A new operator called "cut and splice" is used to replace the traditional crossover operator. In [43], mGA is employed to solve the vehicle routing problem. Kajitani *et al.* [44] proposed a variable length chromosome GA (VGA) for hardware evolution. The cut and splice operators are adopted in VGA to realize recombination. In [45], Srikanth *et al.* proposed a variable-length GA for clustering. Each cluster is approximated by an ellipse and is encoded as a fixed length 0-1 bit string. The chromosome of an individual is allowed to grow or shrink through genetic operators, but the length of the chromosome must be a multiple of the length of a basic element (cluster). Hu and Yang [46] proposed a simple path representation for GA to handle the path planning problem of mobile robots. The robot's environment is given by a set of numbered grids and a path is encoded as a sequence of grid numbers. The first and last element of the sequence denotes the starting point and destination of the path. The number of intermediate nodes may vary from individual to individual. In [47], instead of using the grid numbers to represent the path, each element of the path is given

by a coordinate. Kim and Weck [48] proposed variable chromosome length GA (VCL-GA) to handle the structural topology optimization problem. The algorithm starts from a short chromosome and progressively lengthens the encoding to refine the individuals. Most of the encoding schemes are designed to handle a specific kind of problem and cannot be generalized to tackle the node placement problem.

To overcome the shortcomings, this paper develops a flexible GA (fGA). The proposed fGA adopts a variable-length encoding for chromosomes eligibly to accommodate a variable number of nodes, with new crossover and mutation operators designed accordingly. The encoding of fGA is based on the characteristics of nodes being deployed. Each element (gene) of the encoding has its specific meaning (the coordinates and properties of the nodes). The basic unit of the encoding is a single node and the building blocks of fGA are in the form of partial layouts instead of bit strings. The new crossover, termed subarea-swap crossover, generates offspring by swapping selected subareas of one layout with another. The size and location of the crossover area are dynamically determined by the distribution of nodes. This ensures that the algorithm can be suited for node placement problems with different characteristics. Then, Gaussian mutation is performed on the offspring to adjust nodes positions and properties. Compared to the existing methods, fGA has the following advantages:

1. Automatically adjusting the number of nodes in a legible and efficient manner.

2. Capable of optimizing the nodes' positions and attached properties simultaneously.

3. Enable a fine-grained placement of nodes (since the nodes' positions are not restricted to the predetermined positions).

To investigate the performance of fGA, experiments on two real-world problems (RNP and WFLO) are conducted. The experimental results show that fGA is superior to existing population-based optimization algorithms for NPPs.

The rest of this paper is organized as follows. The NPP is introduced in Section 2. Section 3 provides a detailed description of the proposed flexible genetic algorithm. Experiments on RNP and WFLO problems are presented in Section 4, with thorough analysis of the experimental results. The sensitivity of fGA to the parameter setting is also investigate in this section. Finally, Section 5 gives some concluding remarks and future research directions.

2. Problem Description

NPP is a common and important problem in many engineering fields. In this section, we give a formal description of the problem and provide a discussion on its components. Then, two typical real-world RNP and WFLO problems are briefly described.

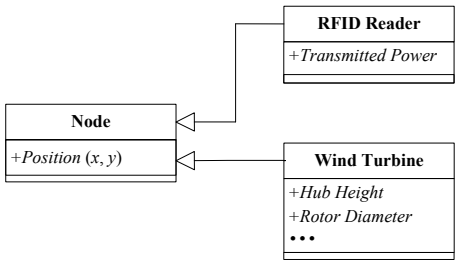

Figure 3: Structures of a Node: An RFID Reader and a Wind Turbine.

2.1. Formulation of the NPP

As its name suggests, the NPP consists of placing a number of nodes in a given area to meet specific requirements optimally. An instance of an NPP can be represented by a five-tuple (A, $Node$, S, F, Ω), where A is the area for placement, $Node$ is the structure of nodes (containing all the properties to be optimized), S is the set of candidate solutions, F is the set of objective functions, and Ω the set of constraints. A candidate solution that satisfies all the constraints is termed a feasible solution. The goal of an NPP solver is to find a feasible solution that yields the best objective values. In the following, we briefly discuss the five components of an NPP.

1) Area for placement. The area for placement can be classified into two types. The first contains a set of discrete points, and the nodes to be placed are restricted to these predetermined points. The second contains a continuous area, where the nodes can be positioned at any locations. Without loss of generality, this paper focuses on the second type. That is, the placement area is enclosed by N_g geometric lines:

$$A = \{(x, y) | g_i(x, y) \geq 0, i = 1, 2, ..., N_g\} \tag{1}$$

2) Characteristics of nodes. A single node is the basic element of an NPP. There are a number of nodes to be deployed. Each node has N_p properties:

$$Node = \{p_i | lb_i \leq p_i \leq ub_i, i = 1, 2, ..., N_p\} \tag{2}$$

(p_1, p_2) is used to represent the position (x, y). lb_i and ub_i are the lower and upper bounds of the i-th property. The behavior of a node depends mostly on how these properties are set. Fig. 3 shows a class diagram of different kinds of nodes in the Unified Modeling Language, where the arrow denotes the generalization (i.e., "is a") relationship. The box on the left represents the basic structure of nodes and those on the right represent two specializations. The basic structure contains the most nontrivial property, namely, the position, while its specializations comprise other properties that also impact on the overall performance, such as the transmitted power of an RFID reader.

Besides, according to whether the properties of nodes are fixed or not, we can divide NPPs into two categories, i.e., homogeneous node placement problems (HoNPPs) and heterogeneous node placement problems (HeNPPs). Compared with an HoNPP, an HeNPP is more flexible, where the properties of each node can be set to any values within given ranges. Hence, the HeNPP is generally more difficult to solve.

3) Candidate solution. A candidate solution comprises a number of nodes. It can be denoted by a set of nodes whose positions are within A:

$$X = \{Node_i | (Node_i.p_1, Node_i.p_2) \in A, i = 1, 2, ..., N_n\} \tag{3}$$

where N_n is the number of nodes in the solution. In the context of NPP, a candidate solution is also termed a layout. We use S to denote the set of all possible layouts.

4) Constraints. We use Ω to denote the set of constraints.

$$\Omega = \{C_i | C_i : Node^{m_i} \rightarrow \{T, F\}, i = 1, 2, ..., N_c\} \tag{4}$$

where N_c is the number of constraints. C_i is an indicator function that maps m_i-fold Cartesian product of *Node* onto Boolean values. The return value T means that the corresponding constraint is satisfied. A candidate solution X is feasible if:

$$\forall i \in [1, N_c], \forall Node_1, ..., Node_{m_i} \in X : C_i(Node_1, ..., Node_{m_i}) = T \tag{5}$$

Most constraints in NPPs impose restriction on the distances between the deployed nodes. For example, WFLO requires that the distances between every two turbines be larger than a certain threshold to avoid damage of the wind turbine blades.

5) Objectives. F is a set of functions that project a layout to a single real value.

$$F = \{f_i | f_i : S \rightarrow \mathbb{R}, i = 1, 2, ..., N_o\} \tag{6}$$

N_o is the number of objectives. The objectives of NPPs vary from problem to problem. Some commonly seen objectives are briefly discussed as follows:

- *Coverage:* Taking WSNs as an example, every node (sensor) has a sensing range. The objective is to cover as many targets as possible with the given number of nodes.
- *Number of nodes:* In practice, the number of nodes for placements is usually not predefined, and it may be difficult to estimate the number of nodes manually. On the premise that other objectives are not disturbed, the fewer nodes, the better the layout is. For some real-world applications where the cost of a node is relatively high, the number of nodes is a critical part in the assessment of a layout.

- *Interference minimization:* Ideally, all the nodes work cooperatively in the area without disturbing one another. However, in a more realistic scenario, there is interference between the deployed nodes. For example, interference arises when several RFID readers interrogate a tag at the same time. This may cause misreading and lower the QoS of an RFID system. Hence, it is necessary to minimize interference when deploying nodes.

- *Other objectives:* There are other objectives that worth mentioning, such as the connectivity between deployed nodes, fault-tolerance and minimal energy consumption in communications.

2.2. Two Typical Real-World NPPs

In this subsection, we briefly discuss two instances of the NPP, i.e., the RNP and WFLO problems. More detailed descriptions of the two problems can be found in [12] and [3] respectively.

1) RFID Network Planning Problem. A typical RFID system is composed of RFID tags, readers, and a host computer system. RFID tags are attached to objects to be identified. RFID readers transmit interrogation signals and receive authentication replies from the tags. The host computer system processes and distributes relevant data. An RFID tag is said to be covered if both reader-to-tag and tag-to-reader communications can be established. The RNP problem consists of placing a number of readers in the working area to cover as many tags as possible while at the same time minimizing the number of deployed readers, interference, and the total transmitted power.

2) Wind Farm Layout Optimization Problem. The WFLO problem is encountered in the design of wind farms. The task is to determine the suitable number of wind turbines to be deployed and the positions of the turbines. If two turbines are placed too close, the power generated by the downwind turbine will decrease significantly due to the existence of wake effects. Wake effects result from the changes in wind speed when wind turbines extract energy from the wind. The goal of an optimizer is to find the optimal deployment that maximizes the power produced and minimizes the cost of wind turbines.

3. Flexible Genetic Algorithm for NPPs

Evolutionary algorithms (EAs) are population-based optimization algorithms inspired by the mechanism of biological evolution. Genetic algorithm (GA) is among the most popular EAs. Owing to its global search ability and robustness, GAs have found widespread real-world applications [49–52]. In the literature, they have been employed to solve some specific instances of NPP [53, 54]. The paper is devoted to the design of a generic approach. Follow the design principles of GAs, we propose a flexible genetic algorithm (fGA) for NPPs. The proposed fGA is distinguished from the existing approaches by its encoding scheme and

genetic operators. In this section, we systematically introduce the algorithmic components of fGA and then present the complete algorithm.

3.1. Genetic Representation

The fGA maintains a population containing *popsize* individuals:

$$POP = \{X_1, X_2, ..., X_{popsize}\} \tag{7}$$

Each individual X_i is a candidate solution (layout) containing a set of nodes:

$$X_i = \{Node_j | (Node_j.p_1, Node_j.p_2) \in A, j = 1, 2, ..., n_i\} \tag{8}$$

$Node_j$ includes all properties to be optimized. n_i is the number of nodes under assessment. We allow the individuals to have different number of nodes. Therefore, n_i is not predefined. It is adjusted in the crossover operator during the search process.

```
Procedure random initialization
01    for i from 1 to popsize
02      X_i←∅;
03      Generate a random number n_i within [1, N_max];
04      for j from 1 to n_i
05            Create a new node Node_j;
06            for k from 1 to N_p
07                  Node_j .p_k=lb_k+(ub_k-lb_k)·rand(0,1);
08            end for
09            X_i←X_i∪{Node_j} ;
10      end for
11    end for
End Procedure
```

Figure 4: Pseudo code of random initialization.

3.2. Initialization

Assuming that no problem-specific knowledge is available, we use random initialization to generate the initial population. For each individual X_i, a random number n_i is generated within the range $[1,N_{max}]$, where N_{max} is the maximum number of nodes. Then, n_i nodes are scattered over the working area. The initial positions of the nodes are randomly sampled from the area. Meanwhile, other properties (if any) are set to random values within their predetermined feasible ranges. The pseudo code of the initialization process is given in Fig. 4.

3.3. Subarea-Swap Crossover

Since a variable-length encoding scheme is used, a location-based subarea-swap crossover independent of the number of nodes, is developed accordingly. Specifically, offspring are generated by swapping partial areas of two parental layouts. Fig. 5 illustrates the crossover operator. The detailed procedures are as follows:

Step 1 For an individual X_i, generate a random number r within [0, 1]. If r is smaller than the crossover probability P_c and X_i contains at least two nodes, go through the operations in Steps 2 and 3 to generate an offspring Y_i. Otherwise, the offspring Y_i is a copy of X_i.

Step 2 Select another individual X_j at random from the population for crossover.

Step 3 Randomly select two nodes from X_i. Calculate the center O of these two nodes and their distance d. Then, draw a circle with center O and radius $d/2$. Draw a corresponding circle with identical location and size in X_j. Swap the contents of the two subareas of X_i and X_j. The resulting layout is retained as offspring Y_i.

The above procedure can be formulated as:

$$Y_i = \begin{cases} X_i \bigotimes X_j, & rand_i < P_c \\ X_i, & \text{otherwise} \end{cases} \tag{9}$$

where $rand_i$ is a random number uniformly distributed in [0, 1], and the operator $\bigotimes$ denotes operations in step 3. To facilitate a better understanding of the process, a pseudo code is provided in Fig. 6. It can be seen that the offspring Y_i may have different number of nodes from its parent X_i when the numbers of nodes in the swapped subareas are different. The adaptive adjustment of the number of nodes relies largely on this crossover operator. Moreover, the subarea-swap crossover has introduced two dynamic features.

1) Locations of crossover areas. The locations of crossover areas are not predefined, but determined by the positions of selected nodes. In this way, crossover areas are automatically adjusted according to the distribution of nodes. No efforts will be wasted on inferior regions that are hardly visited by nodes, and a crossover area is very likely to locate in places where nodes are densely deployed.

2) Sizes of crossover areas. The size of a crossover area is also adaptively adjusted. It depends on the distance between two selected nodes. The diameter of a circular crossover area ranges from d_{min} to d_{max}, where d_{min} denotes the distance of the pair of closest nodes and d_{max} the distance of the pair of farthest nodes. Therefore, the range is determined by the dispersion of the deployed nodes. Large crossover areas increase the population diversity while small crossover areas facilitate fine tuning.

3.4. Mutation

After the crossover operator, the offspring go through Gaussian mutation with probabilities P_m. In this process, the main task is to adjust the nodes properties. The mutation is performed on selected nodes of every individual to fine tune the nodes positions and other properties. Detailed descriptions of the mutation are as follows.

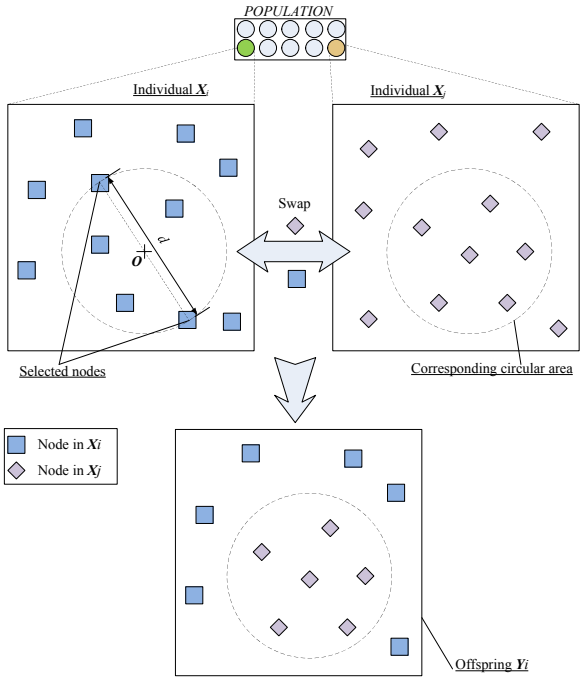

Figure 5: Illustration of crossover operation.

Procedure subarea-swap crossover
01 **for** each individual X_i in the population
02 randomly select another individual X_j ;
03 randomly select two nodes from X_i ;
04 calculate the center O of the two nodes;
05 calculate the distance d between the two nodes;
06 let crossover radius $r = d/2$;
07 offspring $Y_i \leftarrow \emptyset$;
08 **for** each node $Node_k$ in individual X_i
09 calculate the distance d_k between $Node_k$ and O;
10 **if** $d_k \geqslant r$
11 $Y_i \leftarrow Y_i \cup \{Node_k\}$;
12 **end if**
13 **end for**
14 **for** each node $Node_k$ in individual X_j
15 calculate the distance d_k between $Node_k$ and O;
16 **if** $d_k < r$
17 $Y_i \leftarrow Y_i \cup \{Node_k\}$;
18 **end if**
19 **end for**
20 **end for**
End Procedure

Figure 6: Pseudo code of subarea-swap crossover.

For every node in Y_i, generate a random real number r within [0, 1]. If $r < P_m$, then perturbations are performed on the node's properties by adding randomly scaled values. More specifically, for $Node_j$ in Y_i, the mutation is formulated as:

$$Node_j.p_k = Node_j.p_k + N(0, 0.5) \times (ub_k - lb_k), k = 1, ..., N_p \tag{10}$$

where p_k denotes the k-th property of $Node_j$. $N(0, 0.5)$ is a Gaussian random number generator. Variables ub_k and lb_k represent the upper bound and lower bounds of p_k, respectively. N_p is the total number of properties to be optimized.

The utilization of Gaussian perturbation is inspired by evolutionary programming (EP) [55], whose mutation is assisted by a Gaussian random number generator. This kind of mutation is very suitable for NPP for it enables the introduction of diversity adjustments, which greatly increases fGA's local search ability. Note that 1) large perturbation factors cause relatively long jumps, 2) small perturbation factors result in relatively slow progress. Hence, the standard deviation of Gaussian distribution is empirically set to 0.5 to strike a balance. The pseudo code of the mutation operator is shown in Fig. 7.

```
Procedure mutation
01    for each offspring Y_i
02        for each node Node_j in Y_i
03            generate a random number r∈[0,1];
04            if r<Pm
05                for k from 1 to N_p
06                    Node_j .p_k=Node_j .p_k+N(0,0.5)·(ub_k-lb_k);
07                end for
08            end if
09        end for
10    end for
End Procedure
```

Figure 7: Pseudo code of mutation.

3.5. Selection

Selection operator is followed right after the subarea-swap crossover and mutation. Each offspring Y_i originates from two parents X_i and X_j. Since the basic structure of Y_i is inherited from X_i, Y_i is considered as the immediate successor of X_i. For clarity, we name X_i the primary parent of Y_i. In the selection process, Y_i competes with X_i for admission to the next iteration. If the offspring is better than its primary parent, then it survives for the next iteration. Otherwise, the primary parent continues its dominance and the offspring Y_i is discarded. This procedure can be expressed as:

$$X_i = \begin{cases} Y_i, & \text{if } Y_i \text{ is better than } X_i \\ X_i, & \text{otherwise} \end{cases} \tag{11}$$

No additional elitism strategies are required since the best individual will definitely enter the next generation. The selection operator is strong at maintaining the population diversity. Besides the operator described above, other selection operators (e.g., tournament selection and the roulette wheel selection) can also be used.

Crossover, mutation, and selection are repeated until the predefined termination criterion is met. The overall procedure of fGA is summarized as follows:

Step 1 The population goes through the initialization process. In this process, each layout is generated by randomly deploying several nodes in the target area.

Step 2 For each individual X_i in the population, generates an offspring Y_i by performing the subarea-swap crossover on X_i and another randomly selected individual X_j.

Step 3 After the crossover operator, the offspring undergo mutation to search for better layouts through slight adjustments.

Step 4 The offspring are compared with their parents. If the offspring yield better objective values, they take the place of their parents. Otherwise, they are discarded.

Step 5 Test if the termination criterion is met. If the answer is no, go to Step 2, otherwise, end the optimization process and output the best result ever found.

The parameters of fGA include *popsize*, P_c, and P_m. Compared to the conventional GA, no additional parameters are introduced. Overall, fGA preserves the simple structure of GAs and only contains a few parameters.

4. Experimental Tests and Discussions

In this section, we apply the fGA to two real-world problems, i.e., the RNP and WFLO problems. The RNP and WFLO problems have the following features:

1. The best number of nodes to be placed is hard to know. In RNP, the number of nodes is one of the objectives to be optimized, whereas in WFLO, the number of nodes has a direct influence on the fitness. On the other hand, RNP can be viewed as a small-scale problem since the number of nodes (readers) to be included in a layout is relatively small. In comparison, WFLO is considered to be a mid- to large-scale problem.

2. Both problems take into account interference between nodes. In WFLO, interference (wake effect) is a major concern for optimization to reduce power loss. Whereas in RNP, minimizing interference is one of the objectives.

3. RNP falls in the category of HeNPP since the property (transmitted power) of nodes (readers) is adjustable. In contrast, WFLO belongs to HoNPP because it employs the same type of nodes (wind turbines) with fixed properties (hub height, rotor diameter, etc.).

4. The objectives of RNP and WFLO vary significantly. An RNP problem mainly aims at covering more tags, whereas a WFLO aims at capturing more wind energy.

The proposed algorithm is tested on both problems to make our experiments more comprehensive. In the next two subsections, experimental results on both RNP and WFLO problems are presented, followed by a thorough analysis of the results. The algorithm developed in this paper (fGA) was written in C. All the following testing was done on a PC with Intel Core i3-3240 CPU.

4.1. Experiments on RNP

1) Test cases. Twelve test cases [12], namely C30, C50, C100, R30, R50, R100, R30a, R50a, R100a, R30b, R50b, and R100b are used to examine the performance of fGA on RNP. They are based on a 50m×50m working area. Letter 'C' indicates that the tags in the working area are clustered distributed, whereas letter 'R' means uniform distribution of tags. The number behind a letter represents the number of tags included in the working area. It is clear that instances labeled 'R' are harder than those labeled 'C', and more tags included in the working area, more complex the instance is. Therefore, R100, R100a, and R100b are the hardest among the twelve instances.

2) Fitness evaluation. RNP has four objectives, i.e., to maximize the tag coverage, minimize the number of readers, minimize interference, and minimize the sum of the total transmitted power. The objectives are listed in the order of precedence. It is considered that the coverage is the most important objective, followed by the other three one after another. It is an effective way to compare the individuals (solutions) in a hierarchical manner as in [12]. Specifically, when comparing two solutions, we first concentrate on their coverage rates. The one with a higher coverage rate is judged to be better. If the two solutions have the same coverage rate, then the one uses fewer readers is better. The third and fourth objectives are compared accordingly.

3) Algorithms for comparison. The algorithms for comparison are grouped as follows:

G1) GA-16 and GA-25: Two grid-based GAs with elitism strategy, which divide the working area into 4×4 grids and 5×5 grids respectively.

G2) GPSO, VNPSO, and SA-PSO: Three PSO algorithms using fixed-length encoding scheme. GPSO and VNPSO are with global and von Neumann topologies respectively. SA-PSO [56] is a recently proposed algorithm for RNP that incorporates the mechanism of simulated annealing.

Table 1: Notations in the formulation of RNP and their corresponding settings

Symbol	Description	Setting
G_r	gain of reader antenna	6.7dBi
G_t	gain of tag antenna	3.7dBi
T_t	threshold value of tag to build reader-to-tag communication	-14dBm
T_r	threshold value of reader to build tag-to-reader communication	-80dBm
λ	wavelength	0.328m
n	a real number related to environmental conditions	2.2
Γ_{tag}	reflection coefficient	0.8
δ	wireless transmission impairments (cable loss, polarization loss, etc)	2
P_{lb}	Lower bound of reader's transmitted power.	20dBm
P_{ub}	Upper bound of reader's transmitted power.	33dBm

G3) GPSO-RNP and VNPSO-RNP [12]: Two state-of-the-art PSO algorithms with tentative reader elimination for solving RNP.

G4) GA-WMN [53]: A genetic algorithm originally designed for the wireless mesh network planning problem. It is adapted here to tackle the RNP problem.

4) Parameter setting. The notations in the formulation of the RNP [12] and their corresponding settings are summarized in Table 1. The parameters of the fGA are set as follows: *popsize* = 100; $P_c = 0.9$; $P_m = 0.1$. Parameters of GA-16 and GA-25 are set the same as the fGA. The parameters of GA-WMN are set according to [53]. Since GPSO, VNPSO and SA-PSO use fixed-length encoding scheme (as shown in Fig. 1), the number of readers is fixed at $N_{max}/2$. The swarm size is set to 20. The inertia weight is initialized to 0.9 and linearly decreases to 0.4 with respect to iterations. The accelerating coefficients are set as $c_1 = c_2 = 2.0$. Parameters of GPSO-RNP and VNPSO-RNP are set according to [12]. The maximum number of readers available for placement is 12, namely, $N_{max} = 12$. All algorithms terminate after 400,000 fitness evaluations. Each algorithm is run 50 times for each test case to obtain statistically reliable results.

5) Experimental results and discussion. Experimental results on the twelve cases are reported in Tables 2-13. The Wilcoxon rank-sum test (at the 0.05 significance level) is used to determine whether the results obtained by the four groups of algorithms are significantly different from those of the fGA. The statistical reports are listed in the last column of each table. 'Coverage+' indicates that the coverage rate obtained by fGA is significantly higher than the algorithm for comparison. By analogy, 'Reader+' means that the number of deployed readers of fGA is significantly less than the other algorithm. 'Power+' is interpreted in the same way.

The first group of test cases (C30, C50, and C100) contains clustered distributed tags, which is comparatively easy to solve. The experimental results on these cases are given in Tables 2-4. It can be seen that except for GA-25, all the algorithms manage to reach 100% coverage rate at least once. GA-25 fails to reach 100% coverage rate in C30 and C100 in all 50 runs, and the three algorithms based on fixed-length encoding scheme (GPSO, VNPSO, and SA-PSO) fail occasionally in C50 and C100. In comparison, GA-16, GPSO-RNP,

Table 2: Comparison of mean and best results obtained by the algorithms on C30

Case		Mean				Best				Wilcoxon
		Coverage	Readers	Interference	Power	Coverage	Readers	Interference	Power	test
G1	GA-16	100.00%	4	0.000	27.608	100.00%	4	0.000	27.011	Reader+
	GA-25	86.67%	3	0.000	25.360	86.67%	3	0.000	24.774	Coverage+
G2	GPSO	100.00%	6	0.000	35.074	100.00%	6	0.000	31.865	Reader+
	VNPSO	100.00%	6	0.000	34.762	100.00%	6	0.000	31.951	Reader+
	SA-PSO	100.00%	6	0.000	35.096	100.00%	6	0.000	31.872	Reader+
G3	GPSO-RNP	100.00%	3.18	0.000	35.511	100.00%	3	0.000	33.948	Reader+
	VNPSO-RNP	100.00%	3.04	0.000	35.034	100.00%	3	0.000	33.535	Power+
G4	GA-WMN	100.00%	3.03	0.000	34.550	100.00%	3	0.000	33.597	Power+
	fGA	100.00%	3	0.000	33.736	100.00%	3	0.000	33.551	NA

Table 3: Comparison of mean and best results obtained by the algorithms on C50

Algorithm		Mean				Best				Wilcoxon
		Coverage	Readers	Interference	Power	Coverage	Readers	Interference	Power	test
G1	GA-16	100.00%	5.04	0.000	35.213	100.00%	5	0.000	35.266	Power+
	GA-25	100.00%	6	0.000	34.874	100.00%	6	0.000	34.524	Reader+
G2	GPSO	95.60%	6	0.000	35.170	100.00%	6	0.000	31.852	Coverage+
	VNPSO	99.20%	6	0.000	35.023	100.00%	6	0.000	31.742	Coverage+
	SA-PSO	97.60%	6	0.000	35.305	100.00%	6	0.000	31.833	Coverage+
G3	GPSO-RNP	100.00%	5.04	0.000	36.244	100.00%	5	0.000	33.418	Power+
	VNPSO-RNP	100.00%	5.06	0.000	36.565	100.00%	5	0.000	34.522	Reader+
G4	GA-WMN	100.00%	5	0.000	31.927	100.00%	5	0.000	31.896	Power+
	fGA	100.00%	5	0.000	31.816	100.00%	5	0.000	31.729	NA

Table 4: Comparison of mean and best results obtained by the algorithms on C100

Algorithm		Mean				Best				Wilcoxon
		Coverage	Readers	Interference	Power	Coverage	Readers	Interference	Power	test
G1	GA-16	100.00%	8	0.128	36.399	100.00%	8	0.099	36.304	Reader+
	GA-25	99.00%	7.94	1.396	37.658	99.00%	7	1.290	36.159	Coverage+
G2	GPSO	98.34%	6	0.002	38.652	100.00%	6	0.000	37.374	Coverage+
	VNPSO	99.72%	6	0.000	38.167	100.00%	6	0.000	36.803	Coverage+
	SA-PSO	98.33%	6	0.000	38.632	100.00%	6	0.000	37.282	Coverage+
G3	GPSO-RNP	100.00%	5.16	0.000	38.800	100.00%	5	0.000	37.513	Reader+
	VNPSO-RNP	100.00%	5.04	0.000	38.513	100.00%	5	0.000	37.449	Power+
G4	GA-WMN	100.00%	5.33	0.000	36.641	100.00%	5	0.000	36.561	Reader+
	fGA	100.00%	5	0.000	36.479	100.00%	5	0.000	36.342	NA

Table 5: Comparison of mean and best results obtained by the algorithms on R30

Algorithm		Mean				Best				Wilcoxon
		Coverage	Readers	Interference	Power	Coverage	Readers	Interference	Power	test
G1	GA-16	100.00%	8.48	0.063	38.280	100.00%	8	0.103	38.592	Reader+
	GA-25	90.00%	6.18	0.065	35.634	90.00%	6	0.057	34.941	Coverage+
G2	GPSO	92.13%	6	0.000	38.849	100.00%	6	0.000	38.842	Coverage+
	VNPSO	94.53%	6	0.000	38.849	100.00%	6	0.000	38.656	Coverage+
	SA-PSO	90.89%	6	0.000	38.766	96.67%	6	0.000	38.618	Coverage+
G3	GPSO-RNP	99.87%	7.46	0.002	39.821	100.00%	6	0.000	39.265	Reader+
	VNPSO-RNP	100.00%	6.86	0.003	40.143	100.00%	6	0.000	39.574	Reader+
G4	GA-WMN	99.89%	7.37	0.000	37.306	100.00%	6	0.000	37.856	Reader+
	fGA	100.00%	6.26	0.000	37.811	100.00%	6	0.000	37.860	NA

Table 6: Comparison of mean and best results obtained by the algorithms on R50

Algorithm		Mean				Best				Wilcoxon
		Coverage	Readers	Interference	Power	Coverage	Readers	Interference	Power	test
G1	GA-16	100.00%	11	0.051	38.695	100.00%	11	0.043	38.835	Reader+
	GA-25	94.00%	8	0.169	36.081	94.00%	8	0.057	36.743	Coverage+
G2	GPSO	92.52%	6	0.000	39.692	98.00%	6	0.000	40.520	Coverage+
	VNPSO	93.96%	6	0.000	39.690	98.00%	6	0.000	39.595	Coverage+
	SA-PSO	91.87%	6	0.000	39.545	98.00%	6	0.000	40.388	Coverage+
G3	GPSO-RNP	99.84%	8.26	0.012	40.625	100.00%	7	0.000	40.315	Coverage+
	VNPSO-RNP	100.00%	7.66	0.030	40.667	100.00%	7	0.000	40.080	Reader+
G4	GA-WMN	99.93%	8.3	0.000	38.352	100.00%	8	0.000	37.965	Reader+
	fGA	100.00%	7.24	0.004	39.249	100.00%	7	0.000	38.689	NA

Table 7: Comparison of mean and best results obtained by the algorithms on R100

Algorithm		Mean				Best				Wilcoxon
		Coverage	Readers	Interference	Power	Coverage	Readers	Interference	Power	test
G1	GA-16	100.00%	11	0.819	39.395	100.00%	11	0.552	39.759	Reader+
	GA-25	94.00%	9.14	0.676	38.349	94.00%	9	0.406	38.060	Coverage+
G2	GPSO	91.18%	6	0.001	40.074	95.00%	6	0.000	40.098	Coverage+
	VNPSO	94.14%	6	0.001	40.333	97.00%	6	0.044	40.657	Coverage+
	SA-PSO	91.33%	6	0.009	39.961	95.00%	6	0.000	40.782	Coverage+
G3	GPSO-RNP	99.74%	9.24	0.118	41.505	100.00%	8	0.000	40.925	Coverage+
	VNPSO-RNP	100.00%	8.44	0.242	41.462	100.00%	8	0.000	41.031	Reader+
G4	GA-WMN	100.00%	8.97	0.011	39.686	100.00%	8	0.000	39.363	Reader+
	fGA	100.00%	8	0.000	40.094	100.00%	8	0.000	39.660	NA

Table 8: Comparison of mean and best results obtained by the algorithms on R30a

Algorithm		Mean				Best				Wilcoxon
		Coverage	Readers	Interference	Power	Coverage	Readers	Interference	Power	test
G1	GA-16	100.00%	8.07	0.006	35.829	100.00%	8	0.000	35.755	Reader+
	GA-25	86.67%	7.13	0.033	34.551	86.67%	7	0.000	32.260	Coverage+
G2	GPSO	93.44%	6	0.000	38.629	100.00%	6	0.000	38.653	Coverage+
	VNPSO	98.11%	6	0.000	38.635	100.00%	6	0.000	37.632	Coverage+
	SA-PSO	94.89%	6	0.003	38.950	100.00%	6	0.000	37.600	Coverage+
G3	GPSO-RNP	100.00%	6.27	0.003	40.040	100.00%	5	0.000	39.861	Reader+
	VNPSO-RNP	100.00%	6	0.001	40.139	100.00%	6	0.000	39.574	Reader+
G4	GA-WMN	99.89%	6.5	0.000	36.925	100.00%	6	0.000	36.291	Reader+
	fGA	100.00%	5.4	0.000	37.967	100.00%	5	0.000	38.529	NA

Table 9: Comparison of mean and best results obtained by the algorithms on R50a

Algorithm		Mean				Best				Wilcoxon
		Coverage	Readers	Interference	Power	Coverage	Readers	Interference	Power	test
G1	GA-16	100.00%	8.1	0.145	36.983	100.00%	8	0.042	36.791	Reader+
	GA-25	92.00%	8.6	0.215	37.047	92.00%	8	0.140	37.017	Coverage+
G2	GPSO	96.33%	6	0.000	39.669	100.00%	6	0.000	39.073	Coverage+
	VNPSO	98.80%	6	0.000	39.586	100.00%	6	0.000	38.565	Coverage+
	SA-PSO	95.53%	6	0.000	39.468	100.00%	6	0.000	39.210	Coverage+
G3	GPSO-RNP	100.00%	7.17	0.007	40.993	100.00%	6	0.000	40.661	Power+
	VNPSO-RNP	100.00%	7.037	0.009	41.155	100.00%	6	0.000	40.782	Power+
G4	GA-WMN	100.00%	7.37	0.000	38.193	100.00%	7	0.000	37.455	Reader+
	fGA	100.00%	6.67	0.000	37.948	100.00%	6	0.000	37.912	NA

Table 10: Comparison of mean and best results obtained by the algorithms on R100a

Algorithm		Mean				Best				Wilcoxon
		Coverage	Readers	Interference	Power	Coverage	Readers	Interference	Power	test
G1	GA-16	100.00%	10.17	1.191	39.004	100.00%	10	0.878	39.832	Reader+
	GA-25	92.00%	9.77	0.811	38.273	92.00%	9	0.686	37.876	Coverage+
G2	GPSO	92.37%	6	0.012	40.116	97.00%	6	0.000	40.782	Coverage+
	VNPSO	95.70%	6	0.014	40.480	97.00%	6	0.000	40.396	Coverage+
	SA-PSO	92.50%	6	0.013	40.274	98.00%	6	0.000	40.782	Coverage+
G3	GPSO-RNP	96.67%	8.03	0.839	42.284	100.00%	8	0.000	41.489	Coverage+
	VNPSO-RNP	96.67%	8.83	1.008	43.297	100.00%	8	0.000	41.850	Coverage+
G4	GA-WMN	100.00%	8.8	0.003	39.676	100.00%	8	0.000	39.456	Reader+
	fGA	100.00%	8	0.000	39.920	100.00%	8	0.000	39.231	NA

Table 11: Comparison of mean and best results obtained by the algorithms on R30b

Algorithm		Mean				Best				Wilcoxon
		Coverage	Readers	Interference	Power	Coverage	Readers	Interference	Power	test
G1	GA-16	100.00%	8.87	0.003	35.973	100.00%	8	0.000	34.696	Reader+
	GA-25	93.33%	6.4	0.000	33.502	93.33%	6	0.000	33.343	Coverage+
G2	GPSO	96.89%	6	0.000	38.527	100.00%	6	0.000	37.984	Coverage+
	VNPSO	99.33%	6	0.000	38.720	100.00%	6	0.000	37.849	Coverage+
	SA-PSO	98.22%	6	0.000	38.817	100.00%	6	0.000	38.249	Coverage+
G3	GPSO-RNP	100.00%	5.97	0.000	40.036	100.00%	4	0.000	38.817	Reader+
	VNPSO-RNP	100.00%	5.87	0.002	40.090	100.00%	4	0.000	38.875	Reader+
G4	GA-WMN	100.00%	6.1	0.000	36.958	100.00%	5	0.000	37.719	Reader+
	fGA	100.00%	4.13	0.000	38.361	100.00%	4	0.000	38.276	NA

Table 12: Comparison of mean and best results obtained by the algorithms on R50b

Algorithm		Mean				Best				Wilcoxon
		Coverage	Readers	Interference	Power	Coverage	Readers	Interference	Power	test
G1	GA-16	100.00%	10.27	0.110	38.363	100.00%	10	0.092	37.717	Reader+
	GA-25	96.00%	8.67	0.405	37.960	96.00%	8	0.340	37.766	Coverage+
G2	GPSO	95.93%	6	0.003	39.835	100.00%	6	0.000	39.754	Coverage+
	VNPSO	98.07%	6	0.000	39.825	100.00%	6	0.000	39.238	Coverage+
	SA-PSO	95.53%	6	0.000	39.685	100.00%	6	0.000	39.634	Coverage+
G3	GPSO-RNP	100.00%	6.93	0.032	41.040	100.00%	6	0.000	39.901	Reader+
	VNPSO-RNP	100.00%	6.97	0.034	41.066	100.00%	6	0.000	40.078	Reader+
G4	GA-WMN	100.00%	7.9	0.000	38.270	100.00%	7	0.000	38.435	Reader+
	fGA	100.00%	6	0.000	38.942	100.00%	6	0.000	38.532	NA

Table 13: Comparison of mean and best results obtained by the algorithms on R100b

Algorithm		Mean				Best				Wilcoxon
		Coverage	Readers	Interference	Power	Coverage	Readers	Interference	Power	test
G1	GA-16	100.00%	11	0.264	37.962	100.00%	11	0.235	37.871	Reader+
	GA-25	93.00%	10.57	1.967	38.668	93.00%	10	1.816	38.822	Coverage+
G2	GPSO	93.97%	6	0.023	40.103	99.00%	6	0.000	40.622	Coverage+
	VNPSO	97.53%	6	0.005	40.369	99.00%	6	0.000	40.216	Coverage+
	SA-PSO	95.37%	6	0.007	40.193	99.00%	6	0.000	40.391	Coverage+
G3	GPSO-RNP	100.00%	7.8	0.242	41.804	100.00%	7	0.000	41.105	Reader+
	VNPSO-RNP	100.00%	7.9	0.289	41.861	100.00%	7	0.040	41.156	Reader+
G4	GA-WMN	100.00%	8.77	0.004	39.626	100.00%	8	0.000	39.588	Reader+
	fGA	100.00%	7.07	0.033	40.342	100.00%	7	0.000	39.558	NA

VNPSO-RNP, GA-WMN, and fGA have shown their high stability in this group of cases. As reported in Tables 2-4, they achieve the coverage goal in every run. The difference between the results obtained by VNPSO-RNP, GA-WMN, and fGA is moderate. Nevertheless, from the perspective of energy-saving, fGA succeeds in consuming less transmitted power than VNPSO-RNP and GA-WMN.

The second group of test cases (R30, R50, R100, R30a, R50a, R100a, R30b, R50b, and R100b) is more difficult than the first group. The solutions found by GA-16 and GA-25 are inferior to those of GPSO-RNP, VNPSO-RNP, GA-WMN, and fGA. Moreover, since GA-16 and GA-25 are unable to adjust the transmitted power of readers, a noticeable increase in interference is observed. Likewise, the drawback of fixed-length methods emerges while dealing with these cases. GPSO, VNPSO, and SA-PSO fail to reach 100% coverage rate in R50, R100, R100a, and R100b even in their best runs. This is due to the lack of readers. More readers are needed in order to cover the randomly scattered tags. From the results obtained by fGA, it can be inferred that the sufficient (also suitable) numbers of readers are 7, 8, 8, and 7 for R50, R100, R100a, and R100b respectively. The best results are obtained by fGA and VNPSO-RNP. According the mean results and the statistical test, fGA has managed to use fewer readers than VNPSO-RNP and GA-WMN on the premise of full coverage.

Overall, only two algorithms manage to reach 100% coverage in all twelve test cases. They are GA-16 and fGA. However, GA-16 uses a relatively large number of readers, making it inferior to fGA. VNPSO-RNP and GA-WMN are quite promising in solving RNP problems. fGA outperforms VNPSO-RNP and GA-WMN in terms of the number of readers and the total transmitted power.

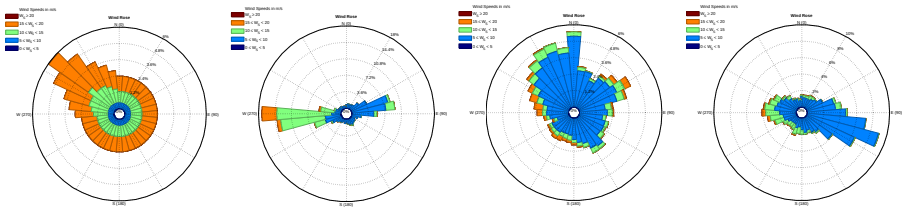

(a) (b) (c) (d)

Figure 8: Wind distribution in test cases c-f. (a) case c (b) case d (c) case e (d) case f.

4.2. Experiments on WFLO

1) Test Cases. It is assumed that turbines are to be placed on a 2000m×2000m wind farm. The occurrence of winds at the wind farm is described using wind roses, which show the strength, direction and frequency of winds. Six test cases are used to examine the performance of fGA. They are listed as follows:

Case a The wind blows from one direction at a constant speed of 12m/s.

Case b The wind has a constant speed of 12m/s and blows from one of 36 possible angles, which range from 0° to 350° in increments of 10°. The wind blows from each angle with an equal possibility.

Case c The wind blows from one of the 36 angles described above. Its speed takes three possible values, i.e., 8m/s, 12m/s, and 17m/s. The probability distribution of wind speed and direction is visualized in Fig. 8(a).

Case d-f The wind direction and speed take the same values as those in Case c. The probability distribution of winds is visualized in Fig. 8(b), (c), (d) respectively.

2) Fitness evaluation. The goal of WFLO is to find a layout that maximizes the power produced and minimizes the cost of wind turbines. The two objectives can be combined into a single fitness value. Specifically, the fitness function is defined as the cost over the power [13]. Intuitively, this gives the cost of a unit of power.

3) Constraint handling. WFLO poses a restriction on the distance of two deployed turbines. To avoid blade damage caused by turbulence, the distance between any two turbines must be at least $5D$, where D is the rotor diameter. An individual may violate the constraint after the crossover and mutation operators. In the proposed fGA, the constraint is handled in a simple way. For the crossover operator, turbines in the crossover area of the first individual are first removed. Then, turbines in the crossover area of the second individual are appended to the first individual one after another. If the introduction of a new turbine will cause violations, then the turbine is excluded. For the mutation operator, if the shift of a turbine will incur blade damage, then the shift is canceled.

Table 14: Notations in the formulation of WFLOP and their corresponding settings

Symbol	Description	Setting
r_r	Rotor radius	20 m
D	Rotor diameter	40 m
z	Hub height	60 m
z_0	Surface roughness	0.3
C_T	Thrust coefficient	0.88

Table 15: Comparison of mean and best results obtained by the algorithms on case a

Algorithm		Mean				Best				Wilcoxon test
		Fitness	Turbines	Cost	Power	Fitness	Turbines	cost	Power	
G1	GA-WFLO	0.001401	41.74	28.508212	20343.53895	0.001388	44	29.838401	21501.7532	+
	BPSO-TVAC	0.001373	42.98	29.229115	21284.06177	0.001372	42	28.650312	20880.72212	+
G2	GPSO	0.001334	50	33.548447	25157.9356	0.001321	50	33.548447	25393.67349	+
	VNPSO	0.001334	50	33.548447	25157.61178	0.001324	50	33.548447	25338.51969	+
G3	RS	0.001313	50	33.548447	25560.36256	0.001307	50	33.548447	25667.29586	+
G4	GA-WMN	0.001307	52.83	35.360606	27045.58975	0.001305	53	35.466523	27170.7361	+
	fGA	**0.001305**	54.44	36.39942	27892.62157	**0.001302**	56	37.413	28730.32948	NA

4) Algorithms for comparison. The algorithms for comparison are grouped as follows:

G1) GA-WFLO [34] and BPSO-TVAC [13]: Two grid-based methods, which divide the wind farm into 10×10 grids.

G2) GPSO and VNPSO: Two PSO algorithms using fixed-length encoding scheme.

G3) SA [57]: A recently proposed random search algorithm for the optimal placement of wind turbines.

G4) GA-WMN [53]: A genetic algorithm originally designed for the wireless mesh network planning problem. It is adapted here to tackle the WFLO problem.

5) Parameter setting. The notations of WFLO [3] and their corresponding settings are listed in Table 14. The parameter settings of fGA, GA-WMN, GPSO and VNPSO are the same as in RNP. GA-WFLO and BPSO-TVAC are set according to [34] and [13] respectively. The maximum number of turbines available for placement is 100, i.e., $N_{max} = 100$. The maximum number of fitness evaluations is set to 100,000. Each algorithm is run 50 times for each test case.

6) Experimental results and discussion. Experimental results of the fGA and the other four algorithms are reported in Tables 15-20. The Wilcoxon rank-sum test is utilized to see if there are significant differences between the results obtained by the fGA and other algorithms. Symbol '+' in the last column indicates the existence of significant difference. In addition, the convergence speed of the algorithms on the six cases are depicted in Fig. 9. The results are averaged over 50 runs.

Case a is a relatively simple case to handle, where the wind blows from one direction and the wind speed is constant. From Table 15, it can be seen that fGA

Table 16: Comparison of mean and best results obtained by the algorithms on case b

Algorithm		Mean				Best				Wilcoxon
		Fitness	Turbines	Cost	Power	Fitness	Turbines	cost	Power	test
G1	GA-WFLO	0.001374	46.84	31.573646	22980.045	0.001371	47	31.668836	23103.1049	+
	BPSO-TVAC	0.001365	48.04	32.317633	23672.30818	0.001364	49	32.917108	24140.49174	+
G2	GPSO	0.001348	50	33.548447	24887.24844	0.001343	50	33.548447	24979.37381	+
	VNPSO	0.001349	50	33.548447	24873.93534	0.001347	50	33.548447	24913.39712	+
G3	RS	0.001357	50	33.548447	24722.52165	0.001349	50	33.548447	24876.17856	+
G4	GA-WMN	0.001341	48.87	32.834979	24490.63152	0.001339	49	32.917108	24580.12842	+
	fGA	**0.001336**	50.02	33.562424	25116.08898	**0.001334**	50	33.548447	25141.2711	NA

Table 17: Comparison of mean and best results obtained by the algorithms on case c

Algorithm		Mean				Best				Wilcoxon
		Fitness	Turbines	Cost	Power	Fitness	Turbines	cost	Power	test
G1	GA-WFLO	0.001327	53.04	35.493836	26753.69232	0.001325	51	34.184054	25789.80437	+
	BPSO-TVAC	0.001322	52.02	34.836398	26358.00784	0.001321	52	34.823538	26361.36445	+
G2	GPSO	0.001315	50	33.548447	25508.28371	0.001314	50	33.548447	25531.75912	+
	VNPSO	0.001315	50	33.548447	25503.70878	0.001315	50	33.548447	25516.99716	+
G3	RS	0.001318	50	33.548447	25448.50594	0.001316	50	33.548447	25488.0407	+
G4	GA-WMN	0.001311	54.57	36.48072	27835.29619	0.00131	55	36.761581	28059.74421	+
	fGA	**0.001309**	55.14	36.853073	28157.71249	**0.001308**	57	38.066615	29099.96617	NA

Table 18: Comparison of mean and best results obtained by the algorithms on case d

Algorithm		Mean				Best				Wilcoxon
		Fitness	Turbines	Cost	Power	Fitness	Turbines	cost	Power	test
G1	GA-WFLO	0.002401	45.27	30.611482	12750.41939	0.002388	46	31.052708	13001.4921	+
	BPSO-TVAC	0.002365	49.27	33.086567	13990.14799	0.002361	50	33.548447	14207.30698	+
G2	GPSO	0.00236	50	33.548447	14212.77597	0.002355	50	33.548447	14243.87585	+
	VNPSO	0.002361	50	33.548447	14209.34714	0.002355	50	33.548447	14245.45122	+
G3	RS	0.002359	50	33.548447	14219.80587	0.002352	50	33.548447	14263.72354	+
G4	GA-WMN	0.002346	50.9	34.121528	14546.73582	0.002343	52	34.823538	14860.43637	+
	fGA	**0.002341**	52.13	34.91032	14911.94289	**0.002338**	53	35.466523	15166.92009	NA

Table 19: Comparison of mean and best results obtained by the algorithms on case e

Algorithm		Mean				Best				Wilcoxon
		Fitness	Turbines	Cost	Power	Fitness	Turbines	cost	Power	test
G1	GA-WFLO	0.003136	48.53	32.626738	10403.66073	0.003131	50	33.548447	10716.1528	+
	BPSO-TVAC	0.003115	49.5	33.232933	10667.72267	0.003113	50	33.548447	10775.76015	+
G2	GPSO	0.003074	50	33.548447	10912.79427	0.003069	50	33.548447	10932.63723	+
	VNPSO	0.003074	50	33.548447	10913.36175	0.003067	50	33.548447	10936.83996	+
G3	RS	0.00309	50	33.548447	10857.60784	0.00308	50	33.548447	10892.38847	+
G4	GA-WMN	0.00306	50.1	33.613133	10984.15514	0.003057	49	32.917108	10767.5412	+
	fGA	**0.003052**	50.93	34.142456	11188.16839	**0.003049**	51	34.184054	11209.74475	NA

Table 20: Comparison of mean and best results obtained by the algorithms on case f

Algorithm		Mean				Best				Wilcoxon
		Fitness	Turbines	Cost	Power	Fitness	Turbines	cost	Power	test
G1	GA-WFLO	0.00313	46.3	31.242234	9981.177752	0.003122	44	29.838401	9558.727848	+
	BPSO-TVAC	0.003088	48.67	32.709462	10592.60216	0.003082	50	33.548447	10883.93689	+
G2	GPSO	0.003073	50	33.548447	10918.92088	0.003067	50	33.548447	10939.42207	+
	VNPSO	0.003073	50	33.548447	10915.91941	0.00307	50	33.548447	10928.76126	+
G3	RS	0.003083	50	33.548447	10883.45863	0.003072	50	33.548447	10921.13958	+
G4	GA-WMN	0.003056	50.13	33.634035	11006.25528	0.003053	50	33.548447	10987.32832	+
	fGA	**0.003047**	50.97	34.163914	11211.44176	**0.003044**	52	34.823538	11441.01969	NA

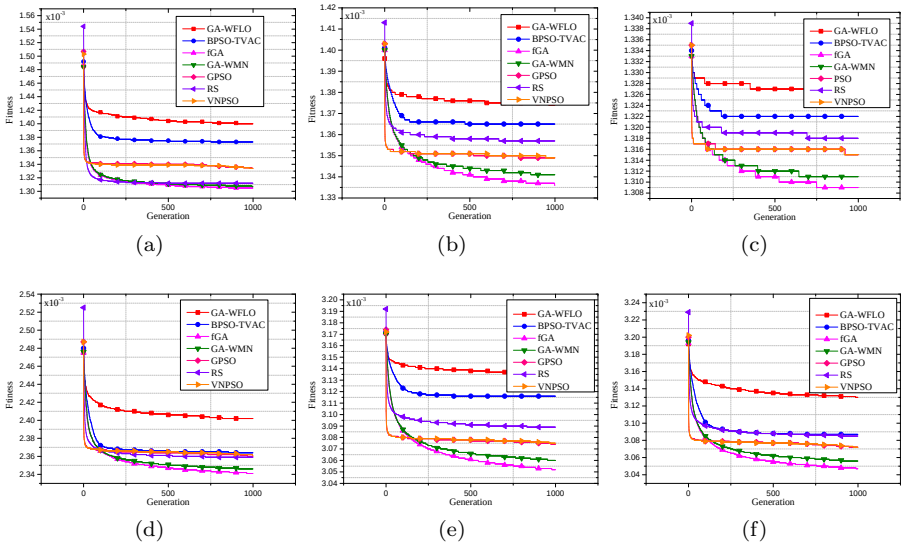

Figure 9: Convergence performance of the algorithms on WFLO cases. (a) case a (b) case b (c) case c (d) case d (e) case e (f) case f.

achieves the best fitness value with a reasonably large number of turbines. The performance of GA-WMN and RS is slightly worse than that of fGA. GPSO and VNPSO perform virtually the same. In comparison, the performance of the two grid-based methods (GA-WFLO and BPSO-TVAC) is in some ways unsatisfactory.

In case b, the average number of turbines obtained by the fGA is 50.02 (reported in Table 16), which is very close to $N_{max}/2$. In this case, it is considered that the methods based on the fixed-length encoding scheme are seen in their best trials, because they are completely free from the task of adjusting the number of turbines and the deficiency is eliminated. However, even though GPSO and VNPSO have a head-start, they are still outperformed by fGA in all 50 runs. The superiority of the fGA owes much to the subarea-swap crossover, which offers a natural way to adjust the number of turbines and at the same time greatly enhance the search ability. The crossover areas are self-adapted according to the distribution of nodes and are therefore more conducive to evolution. In comparison, the two grid-based methods fail to catch up with GPSO, VNPSO, RS, GA-WMN, and fGA.

Compared to the previous two cases, test cases c-f are more practical and complicated. From Tables 17-20, it can be seen that fGA yields the best results among all algorithms. The average number of turbines used by the fGA is larger than those of other algorithms. To make full use of the wind resource, a sufficient number of turbines are needed. Although the installation cost rises as the number of turbines grows, fGA significantly increases the produced power by appropriately deploying the turbines. This way, the results of the fGA turn

485 out to be very promising.

To summarize, in all the six cases of WFLO, the fGA performs the best, followed by GA-WMN, RS, GPSO and VNPSO. In comparison, the performance of the two grid-based methods (GA-WFLO and BPSO-TVAC) is not as good as the fGA. This is mainly due to that, in the grid-based algorithms, the
490 optimization of the positions of nodes is coarse-grained. As the positions for placement are confined to the center of each grid, grid-based methods cannot make the most of the wind farm space. In contrast, fGA, GPSO, and VNPSO are free from this restriction and are able to explore the wind farm completely and thoroughly, leading to more competitive results.

495 Overall, experimental results on RNP and WFLO reveal the drawbacks of previous methods. 1) Grid-based methods are lack of flexibility and are unable to simultaneously optimize the attached properties of nodes. 2) The performance of GPSO and VNPSO can only be guaranteed on the premise that the predefined number of nodes is close to the suitable number. In contrast, the fGA
500 yields relatively good results in both RNP and WFLO. From the experimental results, it can be seen that the fGA is able to automatically adjust the number of nodes and optimize nodes positions and attached properties simultaneously. Its flexibility and efficiency make it a very promising approach for solving different kinds of NPPs.

505 *4.3. Experiments on the Primitive Coverage Problem*

To show the advantage of the proposed algorithm over the existing GA-based node placement approaches, experiments are conducted on a primitive NPP called "coverage problem". The problem is formulated as follows. There are many objects scattered in a working area. The task is to place a number of
510 nodes in the area to cover the objects. Each node has a fixed sensing range. An object is said to be covered by a node if it is in the sensing range of the node. The optimization goal is to cover all the objects by using the least number of nodes. Nine randomly generated test cases are used in the experiment to test the performance of fGA,GA-WMN [53], GA-WFLO [34], and VNPSO-RNP [12].
515 For each test case, 100 objects are scattered randomly in a 100m$\times$100m square area. The sensing radius of nodes is fixed at 10m. The maximum number of fitness evaluations is set to 400,000. The mean results of the algorithms over 50 independent runs are summarized in Table 21. From the table, it can be seen that fGA is able to achieve a 100% coverage rate in all the test cases and the
520 number of deployed nodes is less than those of the other three algorithms. This is attributed to the dynamic feature introduced by the crossover operator, which helps the algorithm to focus its attention on the critical region of the working area. Compared with fGA, the performance of GA-WMN and GA-WFLO is in some sense unsatisfactory. GA-WMN fails to realize full coverage in two of the
525 test cases, while GA-WFLO consumes a larger number of nodes.

4.4. Parameter Investigation

To study the influence of the crossover and mutation probabilities, experiments are conducted on the WFLO problem using different settings of P_c and

Table 21: Comparison of mean results obtained by the algorithms on the coverage problem

Test cases	fGA		GA-WMN		GA-WFLO		VNPSO-RNP	
	Coverage	No. nodes	Coverage	No. nodes	Coverage	No. nodes	Coverage	No. nodes
Case a	**100.00%**	**24.27**	99.97%	25.80	100.00%	37.37	100.00%	31.93
Case b	**100.00%**	**22.90**	100.00%	24.47	100.00%	32.30	100.00%	30.50
Case c	**100.00%**	**22.73**	100.00%	24.50	100.00%	33.07	100.00%	31.37
Case d	**100.00%**	**20.30**	100.00%	23.13	100.00%	31.70	100.00%	28.93
Case e	**100.00%**	**22.10**	100.00%	24.27	100.00%	34.10	100.00%	31.10
Case f	**100.00%**	**22.60**	100.00%	24.93	100.00%	35.13	100.00%	30.03
Case g	**100.00%**	**22.27**	99.93%	24.47	100.00%	35.17	100.00%	30.23
Case h	**100.00%**	**24.23**	100.00%	25.93	100.00%	35.37	100.00%	31.80
Case i	**100.00%**	**22.10**	100.00%	24.30	100.00%	34.37	100.00%	30.13

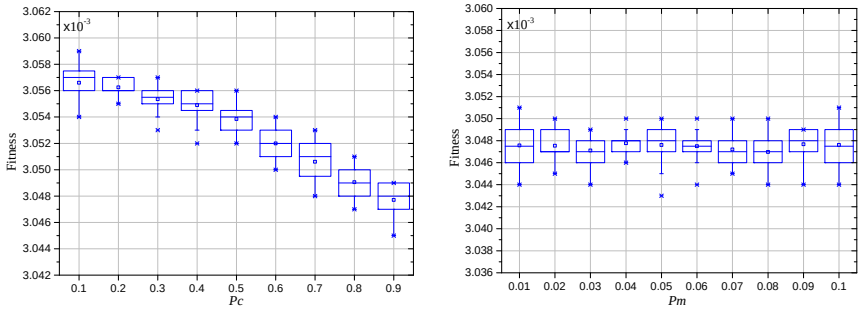

(a) (b)

Figure 10: Effect of the parameter settings. (a) P_c (b) P_m.

P_m. Specifically, the value of P_c ranges from 0.1 to 0.9. As for P_m, values in the interval [0.01, 0.1] are tested. We first investigate the effect of P_c. When studying the influence of P_c, P_m is fixed at 0.1. Subsequently, when testing the effect of P_m, P_c is fixed at 0.9. Experimental results on the test case f are presented in Fig. 10 using box plots. From the figure, it can be observed that fGA with the setting $P_c = 0.9$ is able to achieve the best fitness value. In comparison, fGA is not very sensitive to the setting of P_m. A value between 0.01 and 0.1 is able to provide very stable performance.

5. Conclusion and Future Work

In this paper, we introduce a general framework of node placement problems (NPPs). Further, a flexible algorithm termed fGA is developed to tackle different kinds of NPPs. Compared to the existing approaches, the fGA has several notable features. First, a variable-length encoding scheme is incorporated to enable the automatic adjustment of the number of nodes deployed in the working area. Second, by employing a novel subarea-swap crossover, the fGA is capable of adjusting the number and properties of nodes simultaneously in a natural and efficient manner. For further flexibility, a Gaussian mutation is integrated into the fGA to enhance the search ability through fine adjustments of the nodes.

Experiments have been carried out on two typical NPPs, i.e., RFID network planning and wind farm layout optimization problems, to investigate the performance of the proposed algorithm. The experimental results show that fGA outperforms existing algorithms using a grid-based method or a fix-length method. In dealing with the WFLO problem, fGA is able to find the best fitness values among the compared algorithms. As for the RNP problem, fGA manages to obtain layouts with 100% coverage rates by using the least number of readers. Meanwhile, the layouts produced by fGA also involve lower interference and consume less power than the layouts produced by other algorithms. The results on the two problems reveal that fGA is a promising tool for solving NPPs.

In future research, it would be interesting to apply the fGA to a wider variety of NPPs to further investigate its applicability. According to the 2-D representation scheme, it is noteworthy that the fGA can be adapted to tackle three-dimensional node placement problems, which have received increasing attention in recent years. Moreover, as some NPPs have multiple conflicting objectives, there is a desire to incorporate the fGA with multi-objective optimization techniques to handle multi-objective NPPs.

References

[1] Q. Guan, Y. Liu, Y. Yang, W. Yu, Genetic approach for network planning in the RFID systems, in: Intelligent Systems Design and Applications, 2006. ISDA'06. Sixth International Conference on, volume 2, IEEE, 2006, pp. 567–572.

[2] M. Younis, K. Akkaya, Strategies and techniques for node placement in wireless sensor networks: A survey, Ad Hoc Networks 6 (2008) 621–655.

[3] M. Samorani, The wind farm layout optimization problem, in: Handbook of Wind Power Systems, Springer, 2013, pp. 21–38.

[4] B. Guyaguler, R. Horne, Optimization of well placement, Journal of Energy Resources Technology 122 (2000) 64–70.

[5] A. Konstantinidis, K. Yang, Q. Zhang, D. Zeinalipour-Yazti, A multi-objective evolutionary algorithm for the deployment and power assignment problem in wireless sensor networks, Computer networks 54 (2010) 960–976.

[6] E. L. Lloyd, G. Xue, Relay node placement in wireless sensor networks, Computers, IEEE Transactions on 56 (2007) 134–138.

[7] Y. T. Hou, Y. Shi, H. D. Sherali, S. F. Midkiff, On energy provisioning and relay node placement for wireless sensor networks, Wireless Communications, IEEE Transactions on 4 (2005) 2579–2590.

[8] J. Tang, B. Hao, A. Sen, Relay node placement in large scale wireless sensor networks, Computer communications 29 (2006) 490–501.

[9] H. Chen, Y. Zhu, RFID networks planning using evolutionary algorithms and swarm intelligence, in: Wireless Communications, Networking and Mobile Computing, 2008. WiCOM'08. 4th International Conference on, IEEE, 2008, pp. 1–4.

[10] I. Bhattacharya, U. K. Roy, Optimal placement of readers in an RFID network using particle swarm optimization, International Journal of Computer Networks & Communications 2 (2010) 225–234.

[11] H. Chen, Y. Zhu, K. Hu, T. Ku, RFID network planning using a multi-swarm optimizer, Journal of Network and Computer Applications 34 (2011) 888–901.

[12] Y.-J. Gong, M. Shen, J. Zhang, O. Kaynak, W.-N. Chen, Z.-H. Zhan, Optimizing RFID network planning by using a particle swarm optimization algorithm with redundant reader elimination, Industrial Informatics, IEEE Transactions on 8 (2012) 900–912.

[13] S. Pookpunt, W. Ongsakul, Optimal placement of wind turbines within wind farm using binary particle swarm optimization with time-varying acceleration coefficients, Renewable Energy 55 (2013) 266–276.

[14] Y. Eroğlu, S. U. Seçkiner, Wind farm layout optimization using particle filtering approach, Renewable Energy 58 (2013) 95–107.

[15] Y. Chen, H. Li, K. Jin, Q. Song, Wind farm layout optimization using genetic algorithm with different hub height wind turbines, Energy Conversion and Management 70 (2013) 56–65.

[16] B. Pérez, R. Mínguez, R. Guanche, Offshore wind farm layout optimization using mathematical programming techniques, Renewable Energy 53 (2013) 389–399.

[17] B. Guyaguler, R. N. Horne, et al., Uncertainty assessment of well placement optimization, in: SPE annual technical conference and exhibition, Society of Petroleum Engineers, 2001, pp. 1–13.

[18] W. Bangerth, H. Klie, V. Matossian, M. Parashar, M. F. Wheeler, An autonomic reservoir framework for the stochastic optimization of well placement, Cluster Computing 8 (2005) 255–269.

[19] W. Bangerth, H. Klie, M. Wheeler, P. Stoffa, M. Sen, On optimization algorithms for the reservoir oil well placement problem, Computational Geosciences 10 (2006) 303–319.

[20] K. Chakrabarty, S. S. Iyengar, H. Qi, E. Cho, Grid coverage for surveillance and target location in distributed sensor networks, Computers, IEEE Transactions on 51 (2002) 1448–1453.

[21] J. Wang, N. Zhong, Efficient point coverage in wireless sensor networks, Journal of Combinatorial Optimization 11 (2006) 291–304.

[22] P. Fagerfjäll, Optimizing wind farm layout: more bang for the buck using mixed integer linear programming, Master's thesis, Chalmers University of Technology, Gothenburg University, Gothenburg, Sweden, 2010.

[23] S. Donovan, An improved mixed integer programming model for wind farm layout optimisation, in: Proceedings of the 41st Annual Conference of the Operations Research Society, 2006, pp. 143–151.

[24] M. Nandigam, S. K. Dhali, Optimal design of an offshore wind farm layout, in: Power Electronics, Electrical Drives, Automation and Motion, 2008. SPEEDAM 2008. International Symposium on, IEEE, 2008, pp. 1470–1474.

[25] K. Kar, S. Banerjee, Node placement for connected coverage in sensor networks, in: WiOpt'03: Modeling and Optimization in Mobile, Ad Hoc and Wireless Networks, 2003, pp. 1–2.

[26] W.-C. Ke, B.-H. Liu, M.-J. Tsai, Constructing a wireless sensor network to fully cover critical grids by deploying minimum sensors on grid points is np-complete, IEEE Transactions on Computers 56 (2007) 710–715.

[27] R.-S. Ko, The complexity of the minimum sensor cover problem with unit-disk sensing regions over a connected monitored region, International Journal of Distributed Sensor Networks 2012 (2011) 1–25.

[28] L. Davis, Handbook of genetic algorithms, Bristol and Oxford University Press, 1991.

[29] Y.-J. Gong, W.-N. Chen, Z.-H. Zhan, J. Zhang, Y. Li, Q. Zhang, J.-J. Li, Distributed evolutionary algorithms and their models: A survey of the state-of-the-art, Applied Soft Computing 34 (2015) 286–300.

[30] J. Kennedy, J. F. Kennedy, R. C. Eberhart, Y. Shi, Swarm intelligence, Morgan Kaufmann, 2001.

[31] B. Saavedra-Moreno, S. Salcedo-Sanz, A. Paniagua-Tineo, L. Prieto, A. Portilla-Figueras, Seeding evolutionary algorithms with heuristics for optimal wind turbines positioning in wind farms, Renewable Energy 36 (2011) 2838–2844.

[32] A. P. Bhondekar, R. Vig, M. L. Singla, C. Ghanshyam, P. Kapur, Genetic algorithm based node placement methodology for wireless sensor networks, in: Proceedings of the international multiconference of engineers and computer scientists, volume 1, Citeseer, 2009, pp. 18–20.

[33] G. Mosetti, C. Poloni, B. Diviacco, Optimization of wind turbine positioning in large windfarms by means of a genetic algorithm, Journal of Wind Engineering and Industrial Aerodynamics 51 (1994) 105–116.

[34] S. Grady, M. Hussaini, M. M. Abdullah, Placement of wind turbines using genetic algorithms, Renewable energy 30 (2005) 259–270.

[35] J. S. González, A. G. G. Rodriguez, J. C. Mora, J. R. Santos, M. B. Payan, Optimization of wind farm turbines layout using an evolutive algorithm, Renewable Energy 35 (2010) 1671–1681.

[36] C. Elkinton, J. Manwell, J. McGowan, Algorithms for offshore wind farm layout optimization, Wind Engineering 32 (2008) 67–84.

[37] V. Aristidis, P. Maria, L. Christos, Particle swarm optimization (PSO) algorithm for wind farm optimal design, International Journal of Management Science and Engineering Management 5 (2010) 53–58.

[38] N. A. B. A. Aziz, A. W. Mohemmed, M. Y. Alias, A wireless sensor network coverage optimization algorithm based on particle swarm optimization and voronoi diagram, in: Networking, Sensing and Control, 2009. ICNSC'09. International Conference on, IEEE, 2009, pp. 602–607.

[39] H. Chen, Y. Zhu, K. Hu, Multi-colony bacteria foraging optimization with cell-to-cell communication for RFID network planning, Applied Soft Computing 10 (2010) 539–547.

[40] M. Wagner, K. Veeramachaneni, F. Neumann, U.-M. OReilly, Optimizing the layout of 1000 wind turbines, European wind energy association annual event (2011) 205–209.

[41] J. Kennedy, R. C. Eberhart, A discrete binary version of the particle swarm algorithm, in: Systems, Man, and Cybernetics, 1997. Computational Cybernetics and Simulation., 1997 IEEE International Conference on, volume 5, IEEE, 1997, pp. 4104–4108.

[42] D. Goldberg, K. Deb, B. Korb, Messy genetic algorithms: Motivation, analysis, and first results, Complex systems (1989) 493–530.

[43] K. Tan, T. Lee, K. Ou, L. Lee, A messy genetic algorithm for the vehicle routing problem with time window constraints, in: Evolutionary Computation, 2001. Proceedings of the 2001 Congress on, volume 1, IEEE, 2001, pp. 679–686.

[44] I. Kajitani, T. Hoshino, M. Iwata, T. Higuchi, Variable length chromosome GA for evolvable hardware, in: Evolutionary Computation, 1996., Proceedings of IEEE International Conference on, IEEE, 1996, pp. 443–447.

[45] R. Srikanth, R. George, N. Warsi, D. Prabhu, F. E. Petry, B. P. Buckles, A variable-length genetic algorithm for clustering and classification, Pattern Recognition Letters 16 (1995) 789–800.

[46] Y. Hu, S. X. Yang, A knowledge based genetic algorithm for path planning of a mobile robot, in: Robotics and Automation, 2004. Proceedings. ICRA'04. 2004 IEEE International Conference on, volume 5, IEEE, 2004, pp. 4350–4355.

[47] A. Elshamli, H. A. Abdullah, S. Areibi, Genetic algorithm for dynamic path planning, in: Electrical and Computer Engineering, 2004. Canadian Conference on, volume 2, IEEE, 2004, pp. 677–680.

[48] I. Y. Kim, O. De Weck, Variable chromosome length genetic algorithm for progressive refinement in topology optimization, Structural and Multidisciplinary Optimization 29 (2005) 445–456.

[49] R. Zhang, S. Ong, A. Nee, A simulation-based genetic algorithm approach for remanufacturing process planning and scheduling, Applied Soft Computing 37 (2015) 521–532.

[50] G. H. Costa, F. Baldo, Generation of road maps from trajectories collected with smartphone–a method based on genetic algorithm, Applied Soft Computing 37 (2015) 799–808.

[51] P. Pattanayak, P. Kumar, A computationally efficient genetic algorithm for mimo broadcast scheduling, Applied Soft Computing 37 (2015) 545–553.

[52] S. Karakatič, V. Podgorelec, A survey of genetic algorithms for solving multi depot vehicle routing problem, Applied Soft Computing 27 (2015) 519–532.

[53] R. Pries, B. Staehle, D. Staehle, V. Wendel, Genetic algorithms for wireless mesh network planning, in: Proceedings of the 13th ACM international conference on Modeling, analysis, and simulation of wireless and mobile systems, ACM, 2010, pp. 226–234.

[54] F. Xhafa, C. Sánchez, L. Barolli, Genetic algorithms for efficient placement of router nodes in wireless mesh networks, in: Advanced Information Networking and Applications (AINA), 2010 24th IEEE International Conference on, IEEE, 2010, pp. 465–472.

[55] D. B. Fogel, An introduction to simulated evolutionary optimization, Neural Networks, IEEE Transactions on 5 (1994) 3–14.

[56] M. Tao, S. Huang, Y. Li, M. Yan, Y. Zhou, SA-PSO based optimizing reader deployment in large-scale RFID systems, Journal of Network and Computer Applications 52 (2015) 90–100.

[57] J. Feng, W. Z. Shen, Solving the wind farm layout optimization problem using random search algorithm, Renewable Energy 78 (2015) 182–192.